Broadening, shift and depolarization of broad fine structure alkali spectral lines by helium

E. Roueff, A. Suzor

Classification
Physics Abstracts
5.280

BROADENING, SHIFT AND DEPOLARIZATION OF BROAD FINE STRUCTURE ALKALI SPECTRAL LINES BY HELIUM

E. ROUEFF and A. SUZOR

Département d'Astrophysique Fondamentale, Observatoire de Paris, 92190 Meudon, France

(*Reçu le 2 avril 1974*)

Résumé. — L'écart important de structure fine pour les premiers doublets de résonance de Rb et Cs permet de traiter séparément les niveaux $^2P_{1/2}$ et $^2P_{3/2}$ perturbés par de l'hélium. Dans le cadre des approximations semi-classique et d'impact, les matrices de diffusion $S_{1/2}$ et $S_{3/2}$ sont calculées numériquement avec un modèle de potentiel d'échange, d'abord en négligeant tout couplage $\frac{1}{2} - \frac{3}{2}$, puis par un traitement plus précis qui utilise les potentiels moléculaires et montre que la dépolarisation des raies D_1 est entièrement due au couplage non adiabatique à courte portée.

On examine la validité de résolutions analytiques approchées pour les régions asymptotiques, ainsi que les effets de trajectoire pour les niveaux $^2P_{1/2}$, corrélés à une seule courbe moléculaire ; l'approximation de trajectoire rectiligne s'avère insuffisante pour les phénomènes à très courte portée.

L'accord avec les résultats expérimentaux confirme que l'interaction d'échange est prédominante à moyenne distance.

Abstract. — Due to the large values of the fine structure interval for the first resonance lines of Rb and Cs, we may treat separately the $^2P_{1/2}$ and $^2P_{3/2}$ atomic levels when perturbed by Helium atoms. Within the framework of semi-classical and impact approximations, and assuming an exchange interaction, the diffusion matrices $S^{1/2}$ and $S^{3/2}$ are numerically computed ; firstly by neglecting all $\frac{1}{2} - \frac{3}{2}$ coupling, and secondly, by a more accurate treatment which makes use of the molecular potentials and shows that the D_1-lines depolarization is entirely due to the short range nonadiabatic coupling.

The validity of analytical approximate resolutions for asymptotic regions is studied, and also the trajectory for the $P_{1/2}$ levels, correlated with a single molecular curve ; the rectilinear assumption appears to be insufficient for very short range phenomena.

The agreement with experimental results confirms that the exchange interaction predominates for intermediate distances.

1. **Introduction.** — There is already a considerable amount of literature, both theoretical as well as experimental, concerning alkali rare gas collision effects.

It is only very recently, however, that a complete treatment has been given for the Na-He case within the framework of the semi-classical approximation [1, 4] : fine structure effects and rotational coupling are taken into account in a rigorous manner which involves the solution of systems of coupled differential equations

The interatomic potential used in these papers is the exchange potential model [5, 6] which gives the major contribution to the cross sections. The Van der Waals potential which has been extensively used since a very long time is incomplete when light perturbers such as helium or neon are involved.

In this paper we extend these calculations to the case of the heavy alkalis, for which fine structure splitting is large (see table I). Gordeev, Nikitin and Ovchinnikova [7, 8] have suggested a number of ways of doing this. We have also considered asymptotic situations (small or large impact parameters) where the problem can be simplified.

Let us note briefly the notations and conventions used in this paper. The density of perturbers ($N \simeq 10^{16}$ at.cm^{-3}) is taken to be sufficiently low for the impact approximation to be valid so that we need only consider binary collisions. The perturbers follow in the center of mass system a plane trajectory determined by the spherically symmetric interaction potential. When several potentials are involved, we take a mean rectilinear trajectory.

In the collision plane defined by the trajectory

TABLE I

Atomic level	Fine structure splitting (cm^{-1})
Li 2 P	0.33
Na 3 P	17.19
K 4 P	57.72
Rb 5 P	237.60
Cs 6 P	554.11
Cs 7 P	181.01

and the radiating atom, which is taken as origin for the coordinate system, we choose the Ox axis to be along the initial velocity of the pertuber, and the Oz axis is perpendicular to this plane (see Fig. 1). Using the one electron approximation, we select the electron levels involved by means of the adiabatic criterion (see Mott and Massey [9] for example). We neglect transitions between two levels whose energy difference ΔE is much greater than the inverse of the

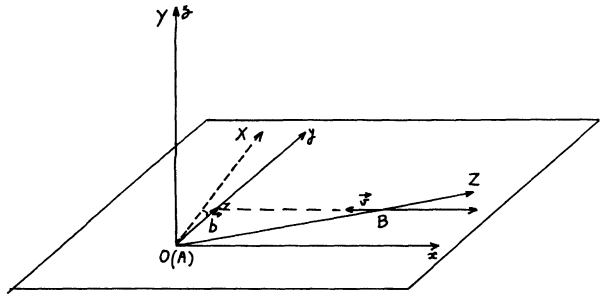

FIG. 1. — $Oxyz$ is the standard frame and $OXYZ$ is the rotating frame where OZ is the internuclear axis.

mean collision time $\tau_c \sim a/v \sim 10^{-12}$ s (v is the mean relative velocity for the temperature $T=450$ K, a the range of the potential, is such that $1/\tau_c$ measures the mean intensity of the collision potential). This is always the case for the alkali and rare gas levels with different (n, 1) quantum numbers, and also for the first fine structure levels of heavy alkalis, which permits us to consider only the angular part of the outer electron wave function.

For the case $\Delta E \ll 1/\tau_c$, we apply the « sudden approximation », in which the terms of the Hamiltonian corresponding to the small ΔE are neglected. This is valid for the Zeeman splitting by magnetic fields $\sim$ 1 T, and also for hyperfine splitting.

2. **The collision treatment.** — 2.1 HAMILTONIAN AND BASIS. —The Halmitonian of the system is written in the following form :

$$\mathcal{H} = \mathcal{H}_A + \mathcal{H}_B + W + V(R)$$

$\mathcal{H}_A$ and $\mathcal{H}_B$ are the electrostatic Hamiltonians of the isolated atoms A and B (the alkali and the perturber respectively), W is the spin orbit Hamiltonian of the alkali, and $V(R)$ is the electrostatic interatomic potential. For the resonant p-states of the alkali, the interatomic potential can be either V_Σ or V_π, depending on the absolute value of the projection (0 or 1) of the orbital momentum of the quasimolecule A-B along the internuclear axis. For the spherically symmetric ground state we have only a Σ potential which we shall call U_0.

Since the fine structure interaction is strong for the involved alkalis, we project the total wave function $|\psi(t)\rangle$ on eigenstates of the angular momentum operator J, in order to satisfy the boundary conditions. Different bases can be used, depending on the manner in which the quantization axis is defined. The most convenient are the following :

— The « standard basis » $|jm\rangle$ where the quantization axis is Oz.

— The « molecular basis » $|jM\rangle$ quantized along the internuclear axis OZ, which leads us to define a « rotating frame » $OXYZ$ with OY along Oz.

This is obtained from the fixed frame $Oxyz$ by means of the geometrical rotation $R(\varphi, \pi/2, \pi/2)$ (φ is the angle (Ox, Oz) at time t, see Fig. 1) which corresponds to rotation matrices $D^{1/2}(\varphi, \pi/2, \pi/2)$ and $D^{3/2}(\varphi, \pi/2, \pi/2)$ within each level.

Two features emerge :

a) When the Schrödinger equation is written in a moving basis (such as the molecular one defined above) we have to take into account the time dependence of the basis itself, and this gives rise to an additional non-adiabatic part of the Hamiltonian :

$$\mathcal{H}_{NA} = -i\frac{d}{dt} = -i\frac{\partial}{\partial\varphi}\frac{d\varphi}{dt} = \dot{\varphi}J_Y . \qquad (1)$$

b) Each term of the Hamiltonian (including the non adiabatic one) is invariant with respect to reflection in the collision plane, and so it will be advantageous to use eigenbases of the reflection operator σ_v. This is true for the $|jm\rangle$ states for the eigenvalues $\pm i$, and this leads to the $\Delta m = 0, \pm 2$ selection rule. The molecular basis, however, is not an eigensystem of the reflection operator ; it is nevertheless possible to find linear combinations of the $|jM\rangle$ states which do satisfy the symmetry property [10].

2.2 INTERACTION MATRICES. — We write the Schrödinger equation in the interaction representation, the term $V(R)$ being put equal to the interaction Hamiltonian. The molecular basis is the most convenient to use since the interaction potential is cylindrically symmetric and independent of electron spin. Rearranging the LS decomposition, the interaction matrices for the ground and excited states in the molecular basis become :

$$\begin{bmatrix} U_0 & 0 \\ 0 & U_0 \end{bmatrix} \qquad (2)$$

$$|\tfrac{1}{2}\tfrac{1}{2}\rangle_Z \qquad |\tfrac{1}{2}-\tfrac{1}{2}\rangle_Z$$

for the ground state, and

$$\left[\begin{array}{cc|cccc} \overline{V} & 0 & 0 & -\frac{\sqrt{2}}{3}\Delta V\,e^{-i\omega t} & 0 & 0 \\ 0 & \overline{V} & 0 & 0 & -\frac{\sqrt{2}}{3}\Delta V\,e^{-i\omega t} & 0 \\ \hline 0 & 0 & \overline{V}-\frac{\Delta V}{3} & 0 & 0 & 0 \\ -\frac{\sqrt{2}}{3}\Delta V\,e^{i\omega t} & 0 & 0 & \overline{V}+\frac{\Delta V}{3} & 0 & 0 \\ 0 & -\frac{\sqrt{2}}{3}\Delta V\,e^{i\omega t} & 0 & 0 & \overline{V}+\frac{\Delta V}{3} & 0 \\ 0 & 0 & 0 & 0 & 0 & \overline{V}-\frac{\Delta V}{3} \end{array}\right] \qquad (3)$$

$$\begin{array}{cccccc} |\tfrac{1}{2}\tfrac{1}{2}\rangle_z & |\tfrac{1}{2}-\tfrac{1}{2}\rangle_z & |\tfrac{3}{2}\tfrac{3}{2}\rangle_z & |\tfrac{3}{2}\tfrac{1}{2}\rangle_z & |\tfrac{3}{2}-\tfrac{1}{2}\rangle_z & |\tfrac{3}{2}-\tfrac{3}{2}\rangle_z \end{array}$$

for the excited one ; we use the notations

$$\Delta V = V_\Sigma - V_\pi \quad \text{and} \quad \overline{V} = \tfrac{1}{3}V_\Sigma + \tfrac{2}{3}V_\pi .$$

The matrix relative to the excited state contains the oscillatory terms $e^{\pm i\omega t}$. Now, the fine structure ω splitting is large, and so it would appear possible that these terms cancel ; however, we shall see below that this would also cancel the depolarization for the D_1 line whose experimental value is in fact ~ 10 Å^2. Thus in order to account for the mutual influence of the $P_{1/2}$ and $P_{3/2}$ states, we include the fine structure Hamiltonian in the expression for the interaction matrix, and diagonalize the whole.

We obtain in this way the eigenenergies of the fixed quasi-molecule A-B, which are called the « adiabatic molecular potentials » [5, 10]. The eigenvalues obtained, which are doubly degenerate due to axial symmetry are given in table II together with the corresponding eigenfunctions. The states are referred to as π and Σ because of their limits at very short distances ($\Delta V \gg \omega$) ; at large distances ($\Delta V \ll \omega$) the adiabatic molecular potentials tend to the atomic levels, $^2P_{1/2}$ for V_1 and $^2P_{3/2}$ for V_2 and V_3 (see table II).

2.3 THE S-MATRICES. — The effect of a particular collision with given **v** and **b** is described by the unitary matrix S which expresses the final state as a function of the initial one :

$$|\psi(+\infty)\rangle = S(\mathbf{b}, \mathbf{v})\,|\psi(-\infty)\rangle$$

TABLE II

Eigenvalues (adiabatic molecular potentials)	Eigenstates (adiabatic molecular states)	Limit for $\Delta V \ll \omega$
$V_1 = \overline{V} + \frac{1}{2}\left[\frac{\Delta V}{3} + \omega - \sqrt{(\Delta V)^2 + \frac{2}{3}\omega\,\Delta V + \omega^2}\right]$	$\left\|\pi \pm \frac{1}{2}\right\rangle = \cos\chi \left\|\frac{1}{2}\pm\frac{1}{2}\right\rangle_z \pm \sin\chi \left\|\frac{3}{2}\pm\frac{1}{2}\right\rangle_z$	$\left\{\begin{array}{l} \left\|\pi\pm\frac{1}{2}\right\rangle \to \left\|\frac{1}{2}\pm\frac{1}{2}\right\rangle_z \\ V_1 \to \overline{V} \end{array}\right.$
$V_2 = \overline{V} + \frac{1}{2}\left[\frac{\Delta V}{3} + \omega + \sqrt{(\Delta V)^2 + \frac{2}{3}\omega\,\Delta V + \omega^2}\right]$	$\left\|\Sigma \pm \frac{1}{2}\right\rangle = -\sin\chi \left\|\frac{1}{2}\pm\frac{1}{2}\right\rangle \pm \cos\chi \left\|\frac{3}{2}\pm\frac{1}{2}\right\rangle_z$	$\left\{\begin{array}{l} \left\|\Sigma\pm\frac{1}{2}\right\rangle \to \left\|\frac{3}{2}\pm\frac{1}{2}\right\rangle_z \\ V_2 \to \overline{V} + \frac{\Delta V}{3} + \omega \end{array}\right.$
$V_3 = \overline{V} - \frac{\Delta V}{3} + \omega = V\pi + \omega$	$\left\|\pi \pm \frac{3}{2}\right\rangle = \left\|\frac{3}{2}\pm\frac{3}{2}\right\rangle_z$	$\left\{\begin{array}{l} \left\|\pi\pm\frac{3}{2}\right\rangle \equiv \left\|\frac{3}{2}\pm\frac{3}{2}\right\rangle_z \\ V_3 \to \overline{V} - \frac{\Delta V}{3} + \omega \end{array}\right.$

Notations : $\Delta V = V_\Sigma - V_\pi$; $\overline{V} = \frac{1}{3}V_\Sigma + \frac{2}{3}V_\Sigma$.

χ is the acute angle defined by the relation $\operatorname{tg} 2\chi = -\dfrac{\frac{2\sqrt{2}}{3}\Delta V}{\omega + \frac{\Delta V}{3}}$.

S is obtained by solving the Schrodinger equation for given boundary conditions. Formally, it is given by :

$$S = \exp\left[- iT \int_{-\infty}^{+\infty} \mathcal{H}_{\text{int}}(t)\, dt \right] \qquad (4)$$

where T is the time ordering operator. Callaway and Bauer [11] have shown that T may be omitted in this expression if, and only if, the commutator

$$\left[\mathcal{H}_{\text{int}}(t), \int_{-\infty}^{t} \mathcal{H}_{\text{int}}(t')\, dt' \right]$$

is zero for all t ; this occurs in particular when $\mathcal{H}_{\text{int}}$ is diagonal.

In other cases the system of coupled differential equations arrising from the Schrödinger equation must be solved numerically. Nevertheless, expression (4) without T does give at least a first order approximation (« scalar solution » [12]) with respect to the interaction Hamiltonian.

2.3.1 *Ground state.* — For the spherically symmetric ground state, the interaction Hamiltonian (2) is scalar. The S matrix is then a phase shift matrix :

$$S = \exp\left[- i \int_{-\infty}^{+\infty} U_0(t)\, dt \right] \times \mathbb{1}$$

and leads to no depolarization for the ground state (see formula (8)). This is confirmed by the very low experimental values, which are less than 10^{-5} Å^2 [13].

2.3.2 *Excited state.* — In our previous discussion, we noted that the excited state may be treated in two different ways. In a first treatment (which we call treatment A) we neglect the non diagonal terms $e^{\pm i\omega t}$ in the matrix (3) and obtain a block for each of the two fine structure levels. After transfering in the standard basis, these blocks become :

$$\mathcal{H}_{\text{int}}^{1/2} = \begin{bmatrix} \overline{V} & 0 \\ 0 & \overline{V} \end{bmatrix} \qquad (5)$$

$$\quad |\tfrac{1}{2}\,\tfrac{1}{2}\rangle_z \quad |\tfrac{1}{2}\,-\tfrac{1}{2}\rangle_z$$

and

$$\mathcal{H}_{\text{int}}^{3/2} = \left[\begin{array}{cc:cc} \overline{V} + \dfrac{\Delta V}{6} & -\dfrac{\Delta V}{2\sqrt{3}} e^{-2i\varphi} & & \\ -\dfrac{\Delta V}{2\sqrt{3}} e^{2i\varphi} & \overline{V} - \dfrac{\Delta V}{6} & \multicolumn{2}{c}{0} \\ \hdashline & & \overline{V} + \dfrac{\Delta V}{6} & -\dfrac{\Delta V}{2\sqrt{3}} e^{2i\varphi} \\ \multicolumn{2}{c:}{0} & -\dfrac{\Delta V}{2\sqrt{3}} e^{-2i\varphi} & \overline{V} - \dfrac{\Delta V}{6} \end{array}\right] \qquad (6)$$

$$|\tfrac{3}{2}\,\tfrac{3}{2}\rangle_z \quad |\tfrac{3}{2}\,-\tfrac{1}{2}\rangle_z \quad |\tfrac{3}{2}\,-\tfrac{3}{2}\rangle_z \quad |\tfrac{3}{2}\,\tfrac{1}{2}\rangle_z$$

The S matrix of the $P_{3/2}$ state is thus obtained by numerically integrating the two corresponding systems of coupled equations. The $P_{1/2}$ state matrix will still be a phase shift matrix leading to no depolarization, as for the ground state.

Let us consider for a more accurate treatment (treatment B) the adiabatic states which we defined above. Their correlations allow us to treat the change of $P_{1/2}$ level within the $|\pi \pm \frac{1}{2}\rangle$ states, whereas the $P_{3/2}$ level is studied in the space of $|\Sigma \pm \frac{1}{2}\rangle$, $|\pi \pm \frac{3}{2}\rangle$; as we noted at the beginning, no real transition $\frac{1}{2} \to \frac{3}{2}$ is considered.

Taking into account the non-adiabatic Hamiltonian, the interaction matrix becomes in the $|\pi \pm \frac{1}{2}\rangle$ basis :

$$\begin{bmatrix} V_1 & iV'_R \\ -iV'_R & V_1 \end{bmatrix}$$

$$|\pi + \tfrac{1}{2}\rangle \quad |\pi - \tfrac{1}{2}\rangle$$

with $\qquad V'_R = \frac{3}{4}\dot{\varphi}(\frac{1}{3} - \cos 2\chi)$.

It is convenient to introduce two new states :

$$\left|\psi \pm \frac{1}{2}\right\rangle = R^{-1(1/2)}\left(\varphi, \frac{\pi}{2}\, \frac{\pi}{2}\right)\left|\pi \pm \frac{1}{2}\right\rangle$$
$$= -\frac{1}{\sqrt{2}} \exp\left(\pm i\frac{\varphi}{2}\right)\left(\left|\pi + \frac{1}{2}\right\rangle \pm i\left|\pi - \frac{1}{2}\right\rangle\right). \qquad (7)$$

They tend to the atomic states $|\frac{1}{2}\, m\rangle$ of the standard configuration in the limit of large R, and are eigenfunctions of the reflexion operator σ_v ; the corresponding interaction matrix is therefore diagonal in this new basis :

$$\begin{bmatrix} V_1 + V_R & 0 \\ 0 & V_1 - V_R \end{bmatrix} \quad \begin{aligned} V_R &= V'_R + \tfrac{1}{2}\dot{\varphi} \\ &= \tfrac{3}{4}\dot{\varphi}(1 - \cos 2\chi) \end{aligned}$$

$$|\psi + \tfrac{1}{2}\rangle \quad |\psi - \tfrac{1}{2}\rangle .$$

This gives rise to an analytical expression for the S matrix, which is still diagonal but no longer scalar and leads to a non vanishing value of the depolariza-

tion cross-section :

$$S=\begin{bmatrix} \exp\left(-i\int_{-\infty}^{+\infty}(V_1+V_R)\,dt\right) & 0 \\ 0 & \exp\left(-i\int_{-\infty}^{+\infty}(V_1-V_R)\,dt\right) \end{bmatrix}$$

The $P_{3/2}$ level is handled in a similar way :

$|\psi \pm \frac{3}{2}\rangle$ and $|\chi \pm \frac{1}{2}\rangle$ are built from the adiabatic $|\pi \pm \frac{3}{2}\rangle$ and $|\Sigma \pm \frac{1}{2}\rangle$ states by the relations :

$$\left|\psi \pm \frac{3}{2}\right\rangle = R^{-1(3/2)}\left(\varphi, \frac{\pi}{2}, \frac{\pi}{2}\right)\left|\pi \pm \frac{3}{2}\right\rangle$$

$$\left|\chi \pm \frac{1}{2}\right\rangle = R^{-1(3/2)}\left(\varphi, \frac{\pi}{2}, \frac{\pi}{2}\right)\left|\Sigma \pm \frac{1}{2}\right\rangle .$$

They reduce to the $|\frac{3}{2}m\rangle$ states of standard configuration in the limit of large R and are still eigenstates of σ_v. Hence $S^{3/2}$ is again obtained directly in the standard basis by solving two systems of only two coupled equations, for which the matrices are :

$$\left[\begin{array}{c|c} V_A & 0 \\ \hline 0 & V_B \end{array}\right]$$

$$|\psi+\tfrac{3}{2}\rangle\,|\chi-\tfrac{1}{2}\rangle \quad |\psi-\tfrac{3}{2}\rangle\,|\chi+\tfrac{1}{2}\rangle$$

$$V_A(V_B) = \tfrac{1}{4}\begin{bmatrix} (V_3+3V_2-4\omega) \pm 6\alpha(4-3\alpha)\dot{\varphi} & \sqrt{3}\,e^{-2i\varphi}\,|\,(V_3-V_2) \mp \alpha(2-3\alpha)\dot{\varphi}\,| \\ \sqrt{3}\,e^{2i\varphi}[(V_3-V_2) \mp \alpha(2-3\alpha)\dot{\varphi}] & (3V_3+V_2-4\omega) \mp 6\alpha^2\dot{\varphi} \end{bmatrix}$$

where $\alpha = \sin^2(\chi/2)$.

3. **Relaxation and broadening constants.** — We consider the effects of collisions with rare gas atoms on the polarization and on the profile of the fluorescence light. In the following paragraph we recall the expressions of the different cross sections involved. Actually, only the mean effect of all collisions is given by the experiments, so that an average over all directions of collisions has to be performed.

3.1 RELAXATION CONSTANTS. — In the case of isotropic collisions, the depolarization of a level j is characterized by $2j+1$ constants when all quenching collisions are neglected. By considering the multipole moments of the density matrix, expanded in terms of the irreducible tensorial sets, we determine the so called relaxation constants γ_k whose expressions were first derived by Omont and Dyakonov and Perel [12, 14] and expressed in terms of the elements $S_{mm'} = \langle jm \mid S \mid jm' \rangle$ of the scattering matrix of the excited state relative to one collision (b impact parameter) :

$$\gamma_k^j = 2\pi N\bar{v}\int_0^\infty P_k^{(j)}(b)\,b\,db$$

where

$$P_k^{(j)}(b) = 1 - \sum_{rr'ss'}(-1)^{r-s}\begin{pmatrix} j & j & k \\ r-r' & & \rho \end{pmatrix}\begin{pmatrix} j & j & k \\ s-s' & & \rho \end{pmatrix} S_{rs}\,S^*_{r's'} .$$

We can also introduce the depolarization cross sections $\sigma_{jm\,jm'}$ (see Masnou and Roueff [3] for example). The relaxation constants have a physical meaning. They follow directly from the experiments (see [35] for example) ; and in particular it is worth noting that owing to the no-quenching condition, γ^0 is zero. However, from a theoretical point of view, the collision mechanisms are more easily discussed by using the depolarization cross sections $\sigma_{mm'}$. In the appendix, we derive the relations between the $\sigma_{mm'}$ and the relaxation cross sections defined by

$$\sigma_k = \frac{1}{N\bar{v}}\gamma_k .$$

Bearing in mind the particular forms we have obtained for the S matrices in the above calculations ($S^{1/2}$ is always diagonal and $S^{3/2}$ composed by two 2×2 diagonal blocks A and B), we shall use the simplified expressions :

$$P_1^{1/2} = \tfrac{1}{3}\,|\,S^{1/2}_{1/2\,1/2} - S^{1/2}_{1/2\,-1/2}\,|^2 \tag{8}$$

$$\begin{cases} P_1^{3/2} = \frac{2}{3} + \frac{4}{15}[|\,A_{12}\,|^2 + |\,B_{12}\,|^2 - \mathrm{Re}\,(A_{22}\,B^*_{22})] - \frac{1}{5}\,\mathrm{Re}\,(A_{12}B^*_{21} + A_{21}\,B^*_{12}) - \frac{1}{5}\,\mathrm{Re}\,(A_{11}\,B^*_{22} + A_{22}\,B^*_{11}) \\ P_2^{3/2} = \frac{1}{5}\times \\ \quad \times[4 + |\,A_{12}\,|^2 + |\,B_{12}\,|^2 + \mathrm{Re}\,(A_{12}\,B^*_{21} + A_{21}\,B^*_{12}) - \mathrm{Re}\,(A_{11}\,B^*_{22} + A_{22}\,B^*_{11}) - \mathrm{Re}\,(A_{11}\,A^*_{22} + B_{11}\,B^*_{22})] \\ P_3^{3/2} = \frac{6}{7} + \frac{1}{35}[|\,A_{12}\,|^2 + |\,B_{12}\,|^2] - \frac{2}{7}\,\mathrm{Re}\,(A_{11}\,B^*_{11}) - \frac{6}{35}\,\mathrm{Re}\,(A_{22}\,B^*_{22}) - \frac{2}{35}\,\mathrm{Re}\,(A_{12}\,B^*_{21} + A_{21}\,B^*_{12}) \\ \qquad - \frac{1}{7}\,\mathrm{Re}\,(A_{11}\,A^*_{22} + B_{11}\,B^*_{22}) - \frac{2}{35}\,\mathrm{Re}\,(A_{11}\,B^*_{22} + A_{22}\,B^*_{11}) . \end{cases} \tag{9}$$

3.2 BROADENING AND SHIFT. — We recall the expressions of the half-width $\gamma = 2w$ and the shift d associated with the lorentzian profile of the line. Adopting the usual conventions (see Tsao and Curnutte [15] for example), we may write

$$I(\omega) = I_0 \frac{w/\pi}{(\omega - \omega_0 - d)^2 + w^2}$$

where

$$w + id = 2\pi N\bar{v} \int_0^\infty \Pi(b)\, bdb\,,$$

and

$$\Pi(b) = 1 - \frac{S_{gr}^{-1}}{(2j+1)} \mathrm{Tr}\,(S_{ex})\,.$$

Owing to the spherical symmetry of the interaction between the perturber and the ground state of the alkaline atoms, the above angular average $\Pi(b)$ is very simple.

It is worth noting that in all these expressions, we have used the mean velocity ($\bar{v} = \sqrt{8\,kT/\pi\mu}$) instead of performing the average over the velocity distribution ; the resulting error is expected to be less than a few percent.

4. **Numerical methods.** — Each of the two steps involved in the numerical computation of the relaxation constants (calculation of $S(b)$ followed by integration over b) was done on the IBM 360-65 computer of the INAG computing center at Meudon Observatory.

4.1 CALCULATION OF THE S MATRICES. — 4.1.1 *Expressions of the potentials.* — Table III gives the analytical expressions obtained from the exchange potential model.

TABLE III

Analytical expressions of the alkali-helium potentials in a.u.

Atomic level	Potential
Cs 6s	$V_\Sigma = U_0 = 0.025\,3\ R^{1.737} \exp(-1.07\ R)$
Cs 6p	$V_\Sigma = \Delta V = 0.008\,4\ R^{2.657} \exp(-0.859\ R)$
Cs 7p	$V_\Sigma = \Delta V = 0.6510^{-4}\ R^{4.745} \exp(-0.593\ R)$
Rb 5s	$V_\Sigma = U_0 = 0.026\,0\ R^{1.608} \exp(-1.108\ R)$
Rb 5p	$V_\Sigma = \Delta V = 0.009\,8\ R^{2.558} \exp(-0.877\ R)$

The V_π potentials of the excited states are zero in this model due to the first order non overlapping of the wave functions.

4.1.2 $P_{1/2}$ *Level.* — We have already found analytical expressions for the $P_{1/2}$ states. In order, therefore, to evaluate the D_1 lines, we need only to compute integrals of the form $\int_{-\infty}^{+\infty} f(t)\,dt$, f being a known function of the internuclear distance R.

The trajectory is determined by the conservation of energy :

$$E = \tfrac{1}{2} mv^2 = \tfrac{1}{2} m(R^2 + R^2\,\dot{\varphi}^2) + V(R)$$

where v is the relative velocity at large distances, V the interaction potential and $\dot{\varphi} = bv/R^2$ the angular velocity.

We find thus the integral

$$\frac{2}{v}\int_{R_T}^{+\infty} \frac{V(R)\,dR}{\sqrt{1 - \dfrac{b^2}{R^2} - \dfrac{V(R)}{E}}}\,,$$

where R_T is the root of the denominator (i. e. the turning point of the classical motion). For a straight line trajectory $R_T = b$. We use the Gaussian quadrature method with 96 points [16] relative to the variable x given by $R = R_T + (1 + x/1 - x)$. In the case of the non rectilinear trajectory we determined the turning point for each value of b by a first approximation method.

4.1.3 $P_{3/2}$ *Level.* — The computer program Merson [17] was used to solve the coupled differential equations involved in the calculations for the 3/2 level. The integration variable $x = \sqrt{R^2 - b^2}$ in the rectilinear trajectory varied between the two values $x = \mp x_\infty$, which correspond to the beginning and the end of the collision (represented by the points at $t = \mp \infty$), and $x_\infty = 30$ a. u. was sufficient in all considered cases. The computing time could be significantly reduced by symmetry considerations since not only does symmetry under reflection reduce the systems to just two coupled equations, but it can also be shown that the S matrix is symmetric for rectilinear motion and is given by [18] :

$$S = U(+\infty, 0)\, U^t(+\infty, 0)$$

due to the time reversal invariance.

It is therefore sufficient to integrate between 0 and x_∞. More over, it is easily shown [19, 20] that when the trace of each 2 × 2 Hamiltonian is substracted, the solution for the initial conditions $\begin{bmatrix} 0 \\ 1 \end{bmatrix}$ can be deduced from that for $\begin{bmatrix} 1 \\ 0 \end{bmatrix}$ by simple transformations which reduce U to the form $\begin{bmatrix} a & -b^* \\ b & a^* \end{bmatrix}$ and so reduces again the integration time by half.

4.2 INTEGRATION OVER THE IMPACT PARAMETER. — This was performed by Simpson's rule up to $b = 20$ or 30 a. u., the contribution of higher values being negligible. Here we must take short integration steps (0.02 a. u.) because the integrands are fast oscillating functions, particularly at short distances. These short range oscillations have no physical meaning since they arise from the rectilinear assumption

which overestimates the phase in the oscillating factors

$$\exp\left(-i\int_{-\infty}^{+\infty}\Delta V\,dt\right).$$

This can be seen clearly on figure 2, where we have plotted the quantity Re $[\Pi^{1/2}(b)]$ (the integrand of the D_1 line broadening) obtained with the two possible trajectories rectilinear and otherwise. Thus, when we take into account the deflection of the trajectory, we obtain not only more reliable results but also an appreciable gain in computing time.

Since the $\frac{3}{2}$ levels involve many potential curves, the $S^{3/2}$ matrices cannot be computed exactly by using a non rectilinear trajectory, at least not within the frame work of this semiclassical treatment.

Nevertheless, to avoid a lengthy and, physically not very significant, solution of the coupled equations at short distances, we evaluated the contribution of collisions with $b < 5$ a. u. by extrapolating the results between 5 and 6 a. u. and also by using the approximate analytical expressions, which we derive below.

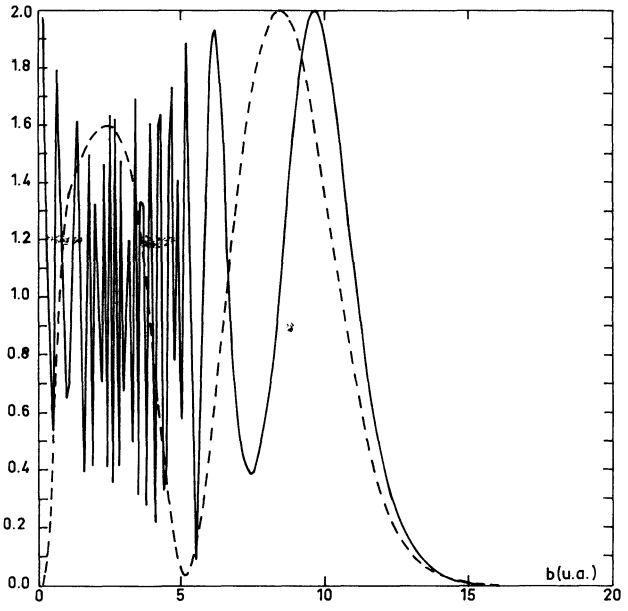

FIG. 2. — Variation of the integrand $\Pi(b)$ of the D_1 line broadening relative to the Cs $6\,^2P_{1/2} \rightarrow 6\,^2S_{1/2}$ transition
——— rectilinear trajectory,
– – – – not rectilinear trajectory.

4.3 ASYMPTOTIC EXPRESSIONS FOR THE INTEGRANDS. — If one term of the Hamiltonian is negligible with respect to the others during most of the collision — i. e. for very small or very large impact parameters — we can find approximate solutions of the Schrodinger equation. This study is most interesting for the D_2 line where no analytical expressions exist. The quantities to be compared are ΔV, ω and $\dot{\varphi}$, since $\overline{V}$ yields only a phase factor in the S matrices.

4.3.1 *Short impact parameters.* — At close distances, ΔV is very much larger than the angular velocity $\dot{\varphi}$. If we write the interaction matrix in the basis of the molecular adiabatic states $|\pi \pm \frac{3}{2}\rangle$, $|\Sigma \pm \frac{1}{2}\rangle$, where the electrostatic interaction appears along the diagonal only, we can neglect the non adiabatic effects, i. e. the non diagonal terms in $\dot{\varphi}$.

We find then in the standard basis :

$$S^{3/2} = R\left(\Phi, \frac{\pi}{2}\frac{\pi}{2}\right)\times$$

$$\times\begin{bmatrix} e^{-i\delta_\pi} & & & \\ & e^{-i\delta_\Sigma} & & 0 \\ & & e^{-i\delta_\pi} & \\ & 0 & & e^{-i\delta_\Sigma} \end{bmatrix} R^{-1}\left(0, \frac{\pi}{2}\frac{\pi}{2}\right) \quad (10)$$

$$|\pi+\tfrac{3}{2}\rangle\,|\Sigma-\tfrac{1}{2}\rangle\,|\pi-\tfrac{3}{2}\rangle\,|\Sigma+\tfrac{1}{2}\rangle$$

where Φ is the angle between the initial and final positions of the OZ axis, and

$$\delta_\pi = \int_{-\infty}^{+\infty}(V_3 - \omega)\,dt, \qquad \delta_\Sigma = \int_{-\infty}^{+\infty}(V_2 - \omega)\,dt.$$

In order to evaluate the effect of trajectory deflection, we may introduce two angles Φ_Σ and Φ_π, relative to the molecular states $\Sigma_{1/2}$ and $\pi_{3/2}$. The splitting $V_2 - V_3 \simeq \Delta V$ is indeed too large at short distances to allow transitions between these two states, and so we may treat them independently, using two distinct trajectories. Hence, the two diagonal blocks which make up the matrix $S^{3/2}$ are :

$$A(B) =$$

$$= e^{-i\delta_\Sigma}\begin{bmatrix} \frac{3}{4}\exp\left(\pm i\frac{3}{2}\Phi_\Sigma\right) & -\frac{\sqrt{3}}{4}\exp\left(\pm i\frac{3}{2}\Phi_\Sigma\right) \\ -\frac{\sqrt{3}}{4}\exp\left(\mp\frac{i}{2}\Phi_\Sigma\right) & \frac{1}{4}\exp\left(\mp\frac{i}{2}\Phi_\Sigma\right) \end{bmatrix}$$

$$+ e^{-i\delta_\pi}\begin{bmatrix} \frac{1}{4}\exp\left(\pm i\frac{3}{2}\Phi_\pi\right) & \frac{\sqrt{3}}{4}\exp\left(\pm i\frac{3}{2}\Phi_\pi\right) \\ \frac{\sqrt{3}}{4}\exp\left(\mp\frac{i}{2}\Phi_\pi\right) & \frac{3}{4}\exp\left(\mp\frac{i}{2}\Phi_\pi\right) \end{bmatrix}.$$

By neglecting all interference between Σ and π states, we obtain the expressions :

$$
\begin{cases}
P_1 = \frac{4}{3} - \frac{1}{3}\cos^2\left(\frac{\Phi_\Sigma}{2}\right) - \frac{3}{5}\cos^2\left(\frac{\Phi_\pi}{2}\right) = \\
\qquad = \frac{4}{3} \text{ for rectilinear motion } (\Phi_\Sigma = \Phi_\pi = \pi) \\
P_2 = \frac{4}{5} + \frac{3}{20}(\sin^2\Phi_\Sigma + \sin^2\Phi_\pi) = \\
\qquad = \frac{4}{5} \text{ for rectilinear motion} \\
P_3 = \frac{8}{7} - \frac{3}{7}\cos^2\left(\frac{\Phi_\Sigma}{2}\right) - \frac{11}{35}\cos^2\left(\frac{\Phi_\pi}{2}\right) + \\
\qquad + \frac{3}{28}(\sin^2\Phi_\Sigma + \sin^2\Phi_\pi) \\
\qquad + \frac{19}{14}\cos\Phi_\Sigma \sin^2\Phi_\Sigma + \frac{1}{14}\cos\Phi_\pi \sin^2\Phi_\pi = \\
\qquad = \frac{8}{7} \text{ for rectilinear motion .}
\end{cases} \tag{11}
$$

The mean values of the broadening and shift integrands are found to be equal to 1 and 0 respectively. This treatment may be called « adiabatic » [20] since the electron is assumed to follow adiabatically the motion of the internuclear axis.

We note that it is not the same as an other « adiabatic approximation » [21, 22] in which the global rotation of the OZ axis is neglected (i. e. the rotation matrices in formula (10)) and which gives :

$$P_1 = \tfrac{1}{2} P_2 = P_3 = \tfrac{2}{5}. \tag{12}$$

In our approximation, we have only neglected the angular velocity $\dot{\varphi}$. We compare the two treatments with the exact calculations in a later part of this paper.

4.3.2 *Large impact parameters.* — Since this time ΔV is always small during such collisions, we use the first order formula (4).

Starting from the interaction matrix (6), we obtain easily (using the method given in (11)) an analytical expression for S, the « scalar solution »

$$S = e^{-i\int_{-\infty}^{\infty} \overline{V}\,dt \begin{bmatrix} A & 0 \\ 0 & B \end{bmatrix}}$$

with

$$A = B = \begin{bmatrix} \cos\xi - iu\frac{\sin\xi}{\xi} & -iv\frac{\sin\xi}{\xi} \\ -iv\frac{\sin\xi}{\xi} & \cos\xi + iu\frac{\sin\xi}{\xi} \end{bmatrix}$$

$$u = \int_{-\infty}^{\infty} \frac{\Delta V}{6}\,dt, \qquad v = \int_{-\infty}^{\infty} -\frac{\Delta V}{2\sqrt{3}} e^{-2i\varphi}\,dt$$

$$(u^2 + v^2) = \xi^2 .$$

This leads to the integrands :

$$P_1^{3/2} = \frac{1}{2} P_2^{3/2} = P_3^{3/2} = \frac{4}{5}\sin^2\xi \leqslant \frac{4}{5}\left[\int_{-\infty}^{\infty} \frac{\Delta V}{3}\,dt\right]^2 . \tag{13}$$

In order to compare the range of the different phenomena, it is interesting to study the way in which the integrands decrease for large b. Taking

$$\alpha = \int_{-\infty}^{\infty} \frac{\Delta V}{3}\,dt$$

as vanishingly small when $b \to \infty$, one finds :

$$P_1^{1/2} \sim \frac{1}{8}\left(\frac{\alpha}{\omega}\right)^4,$$

$$P_1^{3/2} \simeq \frac{1}{2} P_2^{3/2} \simeq P_3^{3/2} \sim \frac{4}{5}\alpha^2 \text{ (see formula (13))} \tag{14}$$

and Re $\Pi(b) \sim \alpha^2/2$, Im $\Pi(b) \sim \alpha$ for the two lines.

5. **Results and discussion.** — The different results obtained are given in tables IV to IX and are compared to some other theoretical and experimental values. The variations of some pertinent integrands are shown in figures 3 and 4, as their behavior is often more useful for the understanding of the collision mechanism than total cross sections and as they also allow the asymptotic formulae to be tested.

TABLE IV

D_1 *line* Cs 6 P-Cs 6 S

	γ/N 10^{-9} rd.s^{-1}.cm^{-3}	d/N 10^{-9} rd.s^{-1}.cm^{-3}	$\sigma_1 = 2\sigma_{1/2\to -1/2}$ Å^2	$\sigma_{opt} = \gamma/Nv$ Å^2
Treatment A	4.58	0.82	0	292
Treatment B rectilinear path	4.76	0.75	17.03	305
Treatment B not rectilinear path	4.71	0.90	10.32	302
Experiments	3.22 [28]		11.8 [29] 6.1 [22]	210

γ and d are the total half width and shift of the line.

σ_1 is the disorientation cross section.

The calculations have been performed for T = 450 K, corresponding to most current experimental conditions.

TABLE V

D_1 *line* Cs 7 P-Cs 6 S

	γ/N 10^{-9} rd.s^{-1}.cm^{-3}	d/N 10^{-9} rd.s^{-1}.cm^{-3}	σ_1 Å^2	σ_{opt} Å^2
Treatment A	19.3	2.72	0	1 232
Treatment B rectilinear path	18.6	2.21	146	1 190
Treatment B not rectilinear path	16.9	2.56	125	1 083
Experiments	18.3 [28] 16.6 [27]	2.83 [27]		1 063 [27]

The notations and the temperature are the same as in table IV.

TABLE VI

D_1 *line* Rb 5 P-Rb 5 S

	γ/N 10^{-9} rd.s^{-1}.cm^{-3}	d/N 10^{-9} rd.s^{-1}.cm^{-3}	σ_1 Å^2	σ_{opt} Å^2
Treatment A	4.07	0.95	0	296
Treatment B rectilinear path	5.02	1.21	28.4	365
Treatment B not rectilinear path	5.02	1.37	23.2	365
Experiments			24.0 [22] 23.0 [24]	
Other theory (Van der Waals)			35.4 [30]	

The notations and the temperature are the same as in table IV.

TABLE VII

D_2 *line* Cs 6 P-Cs 6 S

	γ/N 10^{-9} rd.s^{-1}.cm^{-3}	d/N 10^{-9} rd.s^{-1}.cm^{-3}	σ_1 Å^2	σ_2 Å^2	σ_3 Å^2	$\sigma_{opt} = \gamma/Nv$ Å^2
Treatment A	4.0	0.518	120	150	134	291
Treatment B	4.0	0.513	116	152	136	291
Experiments	2.95 [28]			160 [32]		190 [28]

γ and d are the total half width and shift of the line,
σ_1 is the disorientation cross section,
σ_2 is the disalignment cross section,
σ_3 is the octupole moment cross section.
The calculations have been carried out for $T = 450$ K, corresponding to most current experimental conditions.

TABLE VIII

D_2 *line* Cs 7 P-Cs 6 S

	γ/N 10^{-9} rd.s^{-1}.cm^{-3}	d/N 10^{-9} rd.s^{-1}.cm^{-3}	σ_1 Å^2	σ_2 Å^2	σ_3 Å^2	σ_{opt} Å^2
Treatment A	15.7	1.93	458	630	550	1 006
Treatment B	15.9	2.04	461	629	667	1 020
Experiments	13.0 [27]	1.37 [27]				834 [27]

The notations and the temperature are the same as in table VII.

TABLE IX

D_2 *line* Rb 5 P-Rb 5 S

	γ/N 10^{-9} rd.s^{-1}.cm^{-3}	d/N 10^{-9} rd.s^{-1}.cm^{-3}	σ_1 Å^2	σ_2 Å^2	σ_3 Å^2	σ_{opt} Å^2
Treatment A	3.67	0.514	111	136	121	192
Experiments	3.12 [31]		110 (*)		104 [33]	200 [31]
			95 [33]	118 [33]		
			116 [34]	157 (*)		
Other theory (Van der Waals)			54 [35]	60 [35]	57 [35]	

The notations and the temperature are the same as in table VII.

(*) ELBEL, M., KAMKE, B., SCHNEIDER, W. B. (private communication).

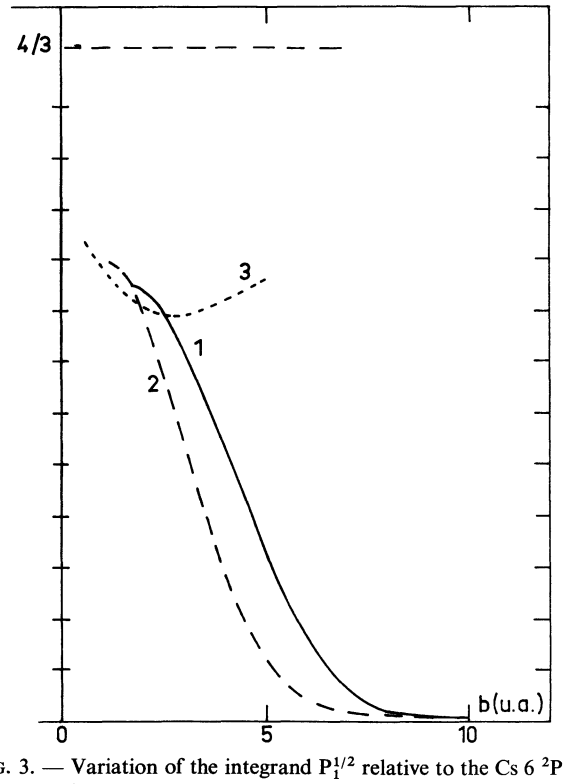

FIG. 3. — Variation of the integrand $P_1^{1/2}$ relative to the Cs 6 $^2P_{1/2}$ disorientation.

——— rectilinear trajectory
— — — not rectilinear trajectory
-------- adiabatic approximation.

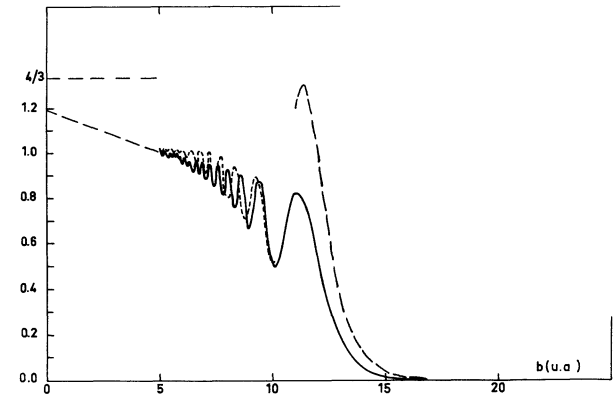

FIG. 4. — Variation of the integrands $P_1^{3/2}$ and $P_2^{3/2}$ relative to the Cs 6 $^2P_{3/2}$ depolarization.

---------- $P_1^{3/2}$ treatment A
——— $P_1^{3/2}$ treatment B
— — — — $P_2^{3/2}$ treatment B (asymptotic region).

5.1 BEHAVIOR OF THE INTEGRANDS. — All the curves have similar shapes except for the case of the D_1 line depolarization. They exhibit first a strong oscillatory part followed by a monotonicaly decreasing region.

Table X shows the ranges of interest for the different phenomena concerning the Cs 6p level (similar conclusions may be drawn for the other cases). It is clear that the depolarization collisions are of shorter range for the $P_{1/2}$ than for the $P_{3/2}$ state,

TABLE X

Cross-section		Impact parameter for which 95 % of the total cross-section is reached (u. a.)	End of the oscillations (u. a.)
	γ	12	9
D_1 line	d	16	11
Cs $6\,^2P_{1/2} \rightarrow 6\,^2S_{1/2}$	σ_1	6	
	γ	13	11.3
D_2 line	d	17	12.4
Cs $6\,^2P_{3/2} \rightarrow 6\,^2S_{1/2}$	σ_1	12.6	10.7
	σ_2	13	11
	σ_3	12.6	10.7

while the shifts are always due to longer range interactions. These different behaviors were predicted analytically by the relations (14).

5.2 TEST OF THE ASYMPTOMATIC FORMULAE. — 5.2.1 *Small impact parameters.* — The predicted mean values of 1 and 0 for Re $\Pi(b)$ and Im $\Pi(b)$ respectively, are well verified. Concerning the relaxation cross sections, it appears that our adiabatic treatment leads to a correct ratio between the P_k (in particular $P_2 < 1 < P_1 < P_3$). This is not true for the other so called adiabatic approximation (see formulae (11) and (12)).

Table XI compares the contribution of collisions with impact parameters smaller than 5 a. u., obtained for σ_1(Cs $6\,^2P_{3/2}$), either by extrapolating the exact calculations or by means of the formulae (11) with the two trajectory assumptions. The three values are not very different which indicates that the effect of trajectory distortion must be rather weak (less than 5 % of the total cross section $\sigma_1 \sim 150$ Å^2).

TABLE XI

	Extrapolation	Adiabatic approximation rectilinear trajectory	Adiabatic approximation not rectilinear trajectory
$2\pi \int_0^5 P_1^{3/2}\, bdb$ Å^2	25	29	24

5.2.2 *Large impact parameters.* — The exact computation shows that the constant ratio between the P_k given by the scalar approximation ($P_1 = \frac{1}{2} P_2 = P_3$) is reached for impact parameters larger than about 12 a. u. for C_S 6p and Rb 5p, 25 a. u. for C_S 7p (for which the potential has a longer range). This feature is of interest because it corresponds to the selection rule $m \nleftrightarrow -m$ (σm, $-m = 0$ see formulae (19)). We insist upon the fact that this rule, arrising from the cylindric symmetry of the electrostatic potential, does not occur at short or intermediate distances because of the non adiabatic effects, although it has been obtained by authors using the above mentionned adiabatic approximation [21, 22].

5.3 DISCUSSION OF BROADENING AND SHIFT RESULTS. — Our results for the half widths are in good agreement with the different experimental values ; in particular, the difference between the D_1 and D_2 components is well respected. The shifts are found to be towards the blue ($d > 0$) as in the experiments, which arrises from the repulsive nature of the exchange potential, whereas the attractive van der Waals forces would yield a red shift. We think however, that the contribution of the van der Waals potential is not negligible for the shifts, due to their long range (table X), which could explain some discrepancies between theoretical and experimental results.

We remark also that the optical cross section $\sigma_{opt} = \gamma/Nv$ is found in all cases to be larger than the relaxation cross sections by a ratio of about 30 for the D_1 lines and 2 for the D_2 lines, in good agreement with the experimental values [23]. This arises from the different nature of the two phenomena, in particular from the ground state contribution to the broadening, while the depolarization involves the excited state only [19, 23].

5.4 DEPOLARIZATION CROSS SECTIONS. — In order to have a valid comparison of the depolarization cross sections, we must ensure that the experiments were performed in presence of a magnetic field H_0 sufficiently strong to decouple the nuclear and electronic angular momenta along the relaxation so that the measurements of the fluorescence radiation yield the pure relaxation times of the electronic observables (which are the computed ones). For experiments performed in weak fields (Hanle effect) we may use the corrective factor calculated by Bulos and Happer [24]. Let us note, moreover, that the octupole cross-section σ_3 is not measured because in all experiments the optical pumping was performed with classical lamps which can not excite multipole moments of order higher than 2 in the vapor.

The relaxation within the excited levels may be explained by two processes. Firstly, the interaction potential splits the $P_{3/2}$ level into two molecular potentials ($\pi_{3/2}$ and $\Sigma_{1/2}$) which undergo different phase shifts during the collision, resulting in transitions between the Zeeman sublevels. This process does not act on the $P_{1/2}$ level whose depolarization is entirely due to a second mechanism, namely the $(\frac{1}{2}, \frac{3}{2})$ mixing which occurs at short distances and

allows the non adiabatic operator to produce a phase shift between the two states $| \pi \pm \frac{1}{2} \rangle$, while it did not act on the « pure » $| \frac{1}{2} \pm \frac{1}{2} \rangle$ substates. By comparing the results of the two treatments, it appears that this second, non adiabatic effect is much less important for the $\frac{3}{2}$ level.

5.5 EFFECT OF THE TRAJECTORY DISTORTION. — The differences between the second and the third lines of tables IV, V, and VI show that, contrary to the case for the D_2 lines, the trajectory distortion has a rather large influence for the D_1 lines, especially for their depolarization. The cross section decreases by about 30 %, the direction of the effect being the expected one since the interaction potential is overestimated when assuming a rectilinear trajectory. The broadening is less affected (10 %) due to the longer range of the phenomenon.

These results are in agreement with previous estimations of Dashevskaya and Mokhova [25] in the case $J = 1$, and show that the rectilinear trajectory assumption, while valid for intermediate range phenomena such as the depolarization of D_2 lines and their broadening, is not good enough when applied to short range processes.

6. **Conclusion.** — The rather good agreement between our results and the experimental ones seems to confirm the validity of the exchange potential model, already verified for lighter alkali atoms (1, 2) in the intermediate range. We must point out here that the constant factor in the analytical expression of the potentials (table III) has a relatively small effect on the results whereas the exponential factors which come from the experimental determination of the binding energy are more critical. It would be interesting however, to re-examine the calculation using more accurate potentials such as the semi-empirical ones numerically calculated by Pascale *et al.* [26].

Appendix : The relationships between the cross-sections $\sigma^{(j)}_{mm'}$ and $\sigma^{(j)}_k$

We propose to clarify the term $(\mathrm{d}\rho/\mathrm{d}t)_{\mathrm{coll}}$ which must be added to the evolution of the mean density matrix $\bar{\rho}$ of the alkali vapour, when mixed with a buffer gas. It has been shown [12] that this term may be written as

$$\frac{\mathrm{d}\rho}{\mathrm{d}t} = - \{ \Gamma \} \bar{\rho} \qquad (15)$$

$\{ \Gamma \}$ is a constant (i. e. independent of time) linear transformation in the Liouville space associated with the atomic states involved, for which $\bar{\rho}$ is a vector, as well as for each operator acting in the atomic states space. When restricted to a given j-level, the dimension of ρ is $(2j + 1)^2$ and two orthonormal bases are of current use ; the first of which is constructed from the diadic operators $| m, m' \gg = | jm \rangle \langle jm' |$, and the second in terms of the irreductible tensor operators T^k_q $(0 \leqslant k \leqslant 2j, - k \leqslant q \leqslant k)$.

1) DEFINITION OF THE CONSTANTS. — Since we restrict ourselves to discussing experiments involving strong magnetic fields, we shall consider only diagonal density matrices ; indeed, even if the optical pumping is able to create coherent states (i. e. non-diagonal terms in $\bar{\rho}$), they disappear in the mean density matrix ρ if the magnetic field is sufficiently strong [36]. Furthermore, one can show [37] that in the general case, provided that the collisions are isotropic, they do not mix the diagonal and non-diagonal terms of $\bar{\rho}$, so that the relaxation of the populations may be studied in exactly the same manner, whether the mean density matrix is diagonal or not.

Thus we stay in the $(2j + 1)$ dimension subspace of ρ constituded by the diagonal operators, which accepts the two bases $| m, m \rangle\rangle$ and T^k_0. If we call $K = [k^{(j)}_{mm'}]$ the matrix of $\{ \Gamma \}$ in the first one, and $G = [\gamma^{(j)}_{kk'}]$ in the second one, we obtain by expanding equation (15) in terms of these two bases :

$$\frac{\mathrm{d}\rho_{mm}}{\mathrm{d}t} = - \sum_{m'} k^{(j)}_{mm'} \rho_{m'm'} \qquad (16)$$

$$\frac{\mathrm{d}\rho^k_0}{\mathrm{d}t} = - \sum_{k'} \gamma^{(j)}_{kk'} \rho^{k'}_0 . \qquad (17)$$

The second system is actually very simple, since the isotropic relaxation is not able to couple different tensorial orders ; $\gamma^{(j)}_{kk'} = \delta_{kk'} \gamma^{(j)}_k$, and G reduces to the diagonal form

$$G = \begin{bmatrix} \gamma_0 & & & \mathrm{O} \\ & & \gamma_1 & \\ & & & \ddots \\ \mathrm{O} & & & \gamma_{2k} \end{bmatrix} .$$

The basis T^k_0, or more generally T^k_q, appears then as the eigenbasis for the relaxation, as for each isotropic phenomenon, and leads to the definition of the $2j + 1$ relaxation cross sections $\sigma^{(j)}_k = \frac{1}{N\bar{v}} \gamma^{(j)}_k$.

In contrast, the $k^{(j)}_{mm'}$ are generally all different from zero ; $(- k_{mm'})$ appears as the transition probability between the sublevels $| jm \rangle$ and $| jm' \rangle$, corresponding to the cross-section $\sigma_{mm'} = \frac{1}{N\bar{v}} (- k_{mm'})$. Physically, this corresponds to the reduction of the number of distinct constants due to the relationships rigorously established in [37] :

$k_{mm'} = k_{m'm}$ (microreversibility)

$k_{mm'} = k_{-m,-m'}$ (isotropy)

$k_{mm} = - \sum_{m' \neq m} k_{mm'}$ (non quenshing assumption).

2) RELATIONSHIPS BETWEEN THE TWO GROUPS OF CONSTANTS. — The definition of the above constants as matrix elements of the relaxation operator $\{\Gamma\}$ enables the relationships between them to be easily derived.

Noting that $\langle\langle A \mid B \rangle\rangle = \mathrm{Tr}(AB^+)$, the scalar product in Liouville space, we can write :

$$\begin{aligned} \mid m, m \rangle\rangle &= \sum_{q,k} \langle\langle T_q^k \mid mm \rangle\rangle T_q^k \\ &= \sum_k \langle m \mid T_0^k \mid m \rangle T_0^k . \end{aligned}$$

We perform in this way a change of basis in the Liouville space, which leads to the relations :

$$\begin{aligned} k_{mm'}^{(j)} &= \langle\langle mm \mid \{\Gamma\} \mid m' m' \rangle\rangle \\ &= \sum_{kk'} \langle m \mid T_0^k \mid m \rangle^* \langle m' \mid T_0^{k'} \mid m' \rangle \times \\ &\qquad \times \langle\langle T_0^k \mid \{\Gamma\} \mid T_0^{k'} \rangle\rangle \\ &= \sum_k \langle m \mid T_0^k \mid m \rangle^* \langle m' \mid T_0^k \mid m' \rangle \gamma_k^{(j)} . \end{aligned}$$

The Wigner-Eckart theorem provides the matrix elements :

$$\langle jm \mid T_0^k \mid jm \rangle = \sqrt{2k+1} \begin{pmatrix} j & k & j \\ -m & 0 & m \end{pmatrix} (-1)^{j-m}$$

(the phase and normalisation of the tensor operators are defined by

$$T_q^k = (-1)^q T_{-q}^{k+} \quad \text{(hence } T_0^k \text{ is hermitian)}$$

and

$$\langle j \mid\mid T^k \mid\mid j \rangle = \sqrt{2k+1}.$$

We thus obtain

$$k_{mm'}^{(j)} = \sum_{k=0}^{2j} (-1)^{2j-m-m'} (2k+1) \times \times \begin{pmatrix} j & k & j \\ -m & 0 & m \end{pmatrix} \begin{pmatrix} j & k & j \\ -m' & 0 & m' \end{pmatrix} \gamma_k^{(j)} .$$

The inverse relationships (γ_k in terms of $k_{mm'}$) are found in the same way :

$$\begin{aligned} \gamma_k^{(j)} &= \sum_{m,m'} \langle jm \mid T_0^k \mid jm \rangle \langle jm' \mid T_0^k \mid jm' \rangle \times \\ &\qquad \times \langle\langle m, m \mid \{\Gamma\} \mid m' m' \rangle\rangle \\ &= (2k+1) \sum_{m,m'} (-1)^{2j-m-m'} \times \\ &\qquad \times \begin{pmatrix} j & k & j \\ -m & 0 & m \end{pmatrix} \begin{pmatrix} j & k & j \\ -m' & 0 & m' \end{pmatrix} k_{mm'}^{(j)} . \end{aligned}$$

For the cases $j = \frac{1}{2}$ and $j = \frac{3}{2}$ we obtain :

$$\boxed{j=\tfrac{1}{2}} \quad \begin{aligned} &\gamma_0 = 0 \\ &\gamma_1 = -2 k_{1/2,-1/2} \text{ or } \sigma_1 = 2 \sigma_{1/2,-1/2} \end{aligned} \tag{18}$$

$$\boxed{J=\tfrac{3}{2}} \quad \begin{cases} k_0 = \frac{1}{20}[-5\gamma_0 + \gamma_1 - 5\gamma_2 + 9\gamma_3] & \gamma_0 = \frac{1}{5}[+3k_0 - 4k_1 + 4k_2 - 3k_3] \\ k_1 = \frac{1}{20}[-5\gamma_0 - 3\gamma_1 + 5\gamma_2 + 3\gamma_3] & \gamma_1 = -\frac{1}{5}[k_0 + 2k_1 + 8k_2 + 9k_3] \\ k_2 = \frac{1}{20}[-5\gamma_0 + 3\gamma_1 + 5\gamma_2 - 3\gamma_3] & \gamma_2 = -2(k_1 + k_2) \\ k_3 = \frac{1}{20}[-5\gamma_0 + 9\gamma_1 - 5\gamma_2 + \gamma_3] & \gamma_3 = -\frac{1}{5}[9k_0 + 8k_1 + 2k_2 + k_3] \end{cases} \tag{19}$$

with the notations :

$$\begin{aligned} k_0 &= -k_{1/2\to -1/2} & k_1 &= -k_{1/2\to 3/2} \\ k_2 &= -k_{1/2\to -3/2} & k_3 &= -k_{3/2\to -3/2} . \end{aligned} \tag{19}$$

Acknowledgements. — The authors would like to thank Professor Elbel for giving them unpublished results. They are also indebted to Doctor Celnikié for critical translation of the manuscript and to Professor Omont for helpful discussions.

References

[1] MASNOU, F., *J. Phys. B.* : *Atom. Molec. Phys.* **3** (1970) 1437.
[2] ROUEFF, E., Thesis (1972), Université de Paris VII.
[3] MASNOU, F., ROUEFF, E., *Chem. Phys. Letters*, **16** (1972) 593.
[4] DELEAGE, J. P., KUNTH, D., TESTOR, G., ROSTAS, F., ROUEFF, E., *J. Phys. B.* : *Atom. Molec. Phys.* **6** (1973) 1892.
[5] NIKITIN, E. E., *J. Chem. Phys.* **43** (1965) 744.
[6] ROUEFF, E., *Astron. and Astrophys.* **7** (1970) 4.
[7, 8] GORDEEV, E. P., NIKITIN, E. E., OVCHINNIKOVA, M., *Can. J. Phys.* **47** (1966) 1819 ; *Opt. and Spectr.* **30** (1971) 189.
[9] MOTT and MASSEY, *The Theory of Atomic Collisions* (Oxford Clarendon Press) 1965.
[10] MASNOU, F., Thesis (1973), Université de Paris VII.
[11] CALLAWAY, J., BAUER, E., *Phys. Rev.* **140A** (1965) 1072.
[12] OMONT, A., *J. Physique* **26** (1965) 26.
[13] ANDERSON, L. W., RAMSEY, A. T., *Phys. Rev.* **132** (1963) 712.
[14] DYAKONOV, M. I., PEREL, V. I., *Sov. Phys. JETP* **21** (1965) 227.
[15] TSAO, C. J., CURNUTTE, B., *J. Quant. Spectrosc. Radiat. Transfer.* **2** (1962) 41.
[16] KOPAL, Z., *Numerical Analysis* (London Chapman and Hall) 1961.
[17] CERNE Program Library.
[18] GAY, J. C., OMONT, A., *J. Physique* **35** (1974) 9.
[19] REBANE, V. N., *Opt. and Spectr.* **26** (1969) 371.
[20] REBANE, V. N., REBANE, T. K., *Opt. and Spectr.* **20** (1966) 101.
[21] WANG, C. H., TOMLINSON, W. J., *Phys. Rev.* **181** (1969) 115.
[22] GALLAGHER, A., *Phys. Rev.* **157** (1967) 68.

[23] EVDOKIMOV, Y. V., KALITEYEVSKII, N. I., *Opt. and Spectr.* **31** (1971) 656.
[24] BULOS, B. R., HAPPER, W., *Phys. Rev.* **A4** (1971) 849.
[25] DASHEVSKAYA, E. I., MOKHOVA, N. A., *Chem. Phys. Letters* **20** (1973) 454.
[26] PASCALE, J., VANDERPLANQUE, J., rapport CEA (1973).
[27] ROSTAS, F., LEMAIRE, J. L., *J. Phys. B.* **4** (1971) 555.
[28] CHEN S. Y., GARRET, R. O., *Phys. Rev.* **144** (1966) 59.
[29] GUIRY, J., KRAUSE, L., *Phys. Rev. A* **6** (1972) 273.
[30] KUMAR, L., CALLAWAY, J., *Phys. Lett.* **28A** (1968) 385.
[31] CHEN, S. Y., *Phys. Rev.* **58** (1940) 1951.
[32] MARKOVA G., *Opt. and Spectr.* **23** (1967) 456.
[33] ZHITNIKOV, R. A., *Sov. Phys. JETP* **31** (1970), 445.
[34] PAPP, J. F., FRANZ, F. A., *Phys. Rev.* **A5** (1972) 1763.
[35] OKUNEVITCH, A. I., PEREL, V. I., *Sov. Phys. JETP* **31** (1970) 356.
[36] BROSSEL, J., *Pompage Optique.* Cours des Houches (1964).
[37] SUZOR, A., Thesis 3e cycle (1973), Université de Paris VII.